Atkin, C.J. Performance trade-off studies for a retrofit Hybrid Laminar Flow Control system. Paper presented at the 2nd AIAA Flow Control Conference, 26 June - 1 July, Portland, Oregon.


CITY UNIVERSITY LONDON

City Research Online

# Performance trade-off studies for a retrofit Hybrid Laminar Flow Control system

Chris Atkin*
*QinetiQ Limited, Farnborough, Hampshire, UK GU14 0LX*

**Recent work in the UK, studying the possible retrofit of a hybrid laminar flow control (HLFC) system to a medium-sized aircraft, is reviewed. The key feature of the work was the use of robust boundary layer tools to design HLFC systems based on direct control of N-factors using a discrete suction chamber technique. The improved HLFC designs were applied to a representative aircraft configuration, leading to a significant reduction in predicted suction mass flow rates, and therefore in pump power requirements and suction system weight. The use of PSE methods to assess suction requirements was further found to reduce predicted suction rates by nearly 25%, increasing the net drag benefit by 10%. Modifications to the wing geometry that were advantageous for laminar flow usually introduced unacceptably large wave drag penalties: the most promising direction for future research therefore appears to be increasing the chord-wise extent of the suction control system. Nevertheless, extrapolating the predicted retrofit HLFC system performance to the entire wing upper surface, tailplane and fin would suggest a potential 6½ - 7% reduction of total aircraft drag for the representative aircraft at cruise.**

## Nomenclature

| | | |
|---|---|---|
| $c_p$ | = | specific heat capacity at constant pressure |
| $C_D$ | = | drag coefficient |
| $C_{L,a/c}$ | = | aircraft lift coefficient |
| $C_{L,sec}$ | = | sectional lift coefficient |
| $C_{L,w+f}$ | = | lift coefficient of wing-fuselage combination |
| $D_{pump}$ | = | effective drag of suction system pump (less exhaust thrust) |
| $u$ | = | velocity |
| $\dot{m}$ | = | suction mass flow rate |
| $M$ | = | Mach number |
| $T$ | = | temperature |
| $p$ | = | pressure |
| $\gamma$ | = | ratio of specific heats |
| $\eta_{a/c}$ | = | overall aircraft efficiency |
| $\eta_{motor}$ | = | efficiency of pump motor |
| $\eta_{off}$ | = | efficiency of engine power off-take process |
| $\eta_{pump}$ | = | overall efficiency of pump |
| $w$ | = | (subscript) at the wing surface |
| $i$ | = | (subscript) at the pump inlet |
| $x$ | = | (subscript) at the pump exhaust |
| $0$ | = | (subscript) stagnation conditions |
| $\infty$ | = | (subscript) in the free stream |

* QinetiQ Fellow, Future Systems and Technology Division, Küchemann Building. Member AIAA.

# I. Introduction

THE delay of laminar-turbulent transition remains one of the most promising routes to significant reductions in aircraft drag, but a practical and cost-effective implementation of laminar flow control has apparently yet to be identified. Flow control by the use of suction through porous wing skins seems in particular to be dogged by the need for heavy and power-hungry systems which consume much of the performance benefit arising from the reduction in friction drag.

The work presented in this paper was carried out at QinetiQ (formerly DERA) in the UK as part of the European 4th Framework HYLTEC (**HY**brid **L**aminar flow **TEC**hnology) project[1-3] between 1997 and 2000. One of the objectives of the HYLTEC project was to consider the possibility of introducing Hybrid Laminar Flow Control (HLFC) as a retrofit to a classically-designed turbulent wing, the idea being that the risks associated with an incremental approach would be modest enough to encourage the gradual introduction of the technology, albeit with modest gains in performance. This is in contrast to the often-proposed optimized HLFC aircraft with reduced sweep, wing loading and operating altitude — a concept so revolutionary as to be guaranteed a permanent place in the archives of the Future Projects Office.

A second objective of the current work was to establish exactly what improvements were required from the aerodynamic design to push HLFC technology towards application: at that time it was often said that the aerodynamic design was well understood and that the real problems lay with the system design.

# II. Suction chamber layout for an HLFC system

## A. Review of classical aerodynamic HLFC system design

The aerodynamic design of HLFC systems focuses mainly on two questions: where to apply suction, and how much suction to apply. The first phase of the work at QinetiQ was concerned with increasing the precision of this specification process to enable parametric configuration studies to be carried out in a scientific manner[2].

At the start of the project, the existing approach to the specification of the HLFC suction system involved defining a relatively simple distribution of suction velocity. An example of this would be a trapezium-shaped distribution between fixed chordwise positions as illustrated in Fig. 3. The specification process would then be simplified to the specification of the total suction rate and the slope of the trapezium rooftop. More complex distributions have been tried (e.g. a trapezium followed by a rectangle) but the simple trapezium has proved quite effective: it observes simple practical constraints (for example that the suction system cannot extend into the main wing box) and encapsulates early design experience, now supported by modern adjoint sensitivity methods, that suction is more efficient towards the wing leading edge, where instability first occurs.

The required shape and size of the trapezium can be determined using a linear $e^N$ stability analysis of the laminar boundary layer over the relevant part of the wing. Although linear stability analysis lacks key ingredients required for the accurate prediction of transition (such as the physics of receptivity and non-linear mechanisms) it can be used effectively for the modelling of transition control where the control technique operates on small-amplitude disturbances. Semi-empirical criteria can also be found which define the limits of applicability of such an approach, as will be shown later. The methods used to obtain the results reported in this paper were developed at QinetiQ and its predecessor organizations and are in use throughout UK academia and industry for these sorts of applications. The swept-tapered laminar boundary layer method 'BL2D'[4] is based on the approach of Horton and Stock[5] and has been shown to perform well on poorly-resolved and uneven experimental pressure distributions. The stability analysis method 'CoDS'[6] is based on the spatial approach of Mack[7] and has been developed into a 'black-box' tool. Without any user input requirement, the method finds and analyses instability modes over a range of frequencies and propagation angles: spurious eigenvalues are returned with a frequency of less than 1 in $10^8$. The combination of the two methods provides an extremely robust and user-friendly capability for HLFC design.

The use of these tools is demonstrated in Figures 1-4. Figure 1 illustrates a typical pressure distribution for a mid-span section of a high-aspect-ratio swept-tapered transport aircraft wing under transonic (Mach ~ 0.8) cruise conditions: this pressure distribution was used for the majority of the HLFC analysis presented in this paper, although cases generating 20% more and less lift respectively were also analyzed without special treatment. The other characteristics chosen for the baseline aircraft were a chord Reynolds number of about 30 million (at mid-span) and a leading edge sweep of about 32°. We also assume that the attachment line transition problem has been controlled in a suitable manner. Applying a boundary layer and $e^N$ stability analysis to the upper surface of this wing section at yields a set of N-factor curves as shown in Fig. 2. For the purposes of demonstrating the design technique we here consider all modes to be dangerous and we also use the classical two-dimensional criterion that transition occurs near N = 9: a number of alternative strategies have been tested in Europe[8] and there is, of course, nothing to

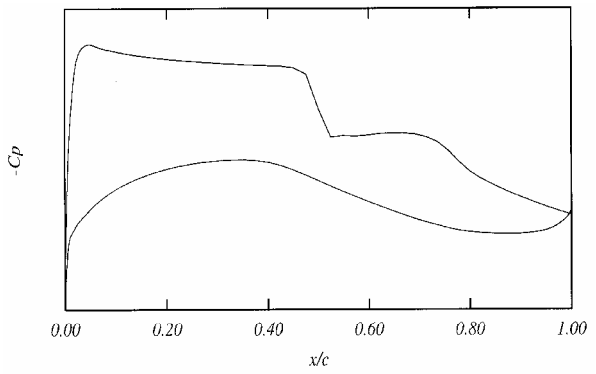


**Figure 1. Mid-span section pressure distribution adopted for the HYLTEC specimen aircraft.**

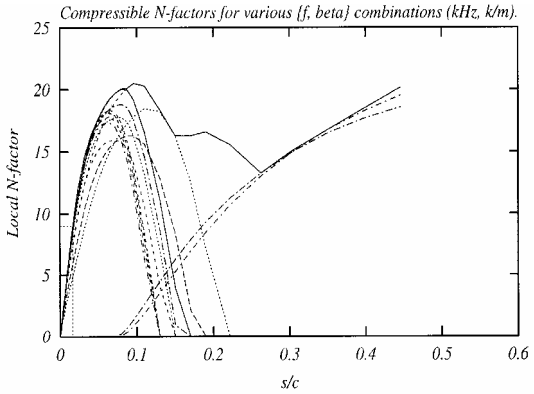


**Figure 2. N-factors corresponding to pressure distribution in Fig. 1 (without surface suction).**

stop the techniques described in this paper from being coupled with any other $e^N$ strategy. Figure 2 therefore shows the 'envelope' curve of the maximum N-factor across all modes, Tollmien-Schlichting (TS) and both stationary and travelling crossflow (CF) modes. Note that x-axis of this figure shows developed surface distance *s/c*: this co-ordinate is a good deal more informative about leading edge transition than *x/c*. Applying the N = 9 criterion to this envelope curve, one would expect transition to occur very close to the leading edge. Additionally, some individual modal N-factor curves (which contribute to the locus of the envelope) are shown to highlight the apparent separation of the CF (leading edge) and TS (mid-chord) dominance. This is a feature of the adverse-pressure-gradient rooftop shown in Fig. 1 and is not usually observed with classical laminar flow sections. The latter tend to employ favourable pressure gradients to stabilize TS modes: favourable pressure gradients on swept wings also prolong the region of CF instability, and are often used in experimental investigations of CF modes for that reason. No results are seen in Fig. 2 beyond 45% chord, where a laminar boundary layer would separate under the influence of the shock wave.

Figure 3 illustrates the application of a trapezoidal transpiration distribution to this wing section: suction is limited to the leading edge ahead of 17% chord (which here equates to about *s/c* = 0.19) and the ratio of suction magnitude at the upstream and downstream limits is here fixed at 2:1. The transpiration rates in Fig. 3 are expressed as suction hole velocities, which are determined using a notional surface porosity (for the purposes of comparison with later results). The overall mass flow rate is adjusted to limit the 'envelope' N-factor in the suction region to 5 or less and transition is seen to move aft of 30% chord, although persisting with an N = 9 criterion downstream of a porous panel would be an optimistic view: more normally a slightly reduced transition threshold would be used to reflect the introduction of disturbances by the porous suction surface. Additional suction ahead of *s/c* = 0.19 would add little (and prove costly, as will be seen later), whereas allowing N-factors to attain values close to the critical 'transition' value would be straying outside the bounds of applicability of the linear $e^N$ technique. Of course, the precise value of this 'control' N-factor is unknown and has never been explicitly investigated — however it must be a mandatory feature of using linear $e^N$ for suction system design, as the suction system specification is extremely sensitive to the chosen value. We note immediately that this topic requires further experimental research.

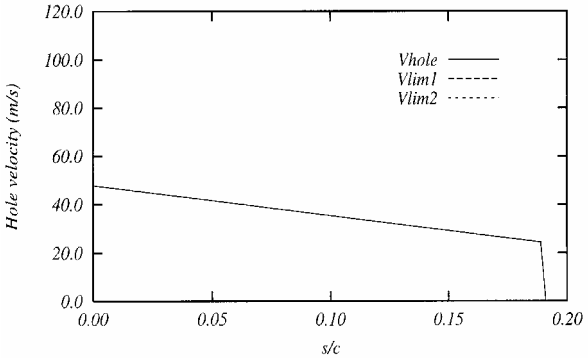


**Figure 3. Trapezium suction distribution used to control leading-edge crossflow instability.**

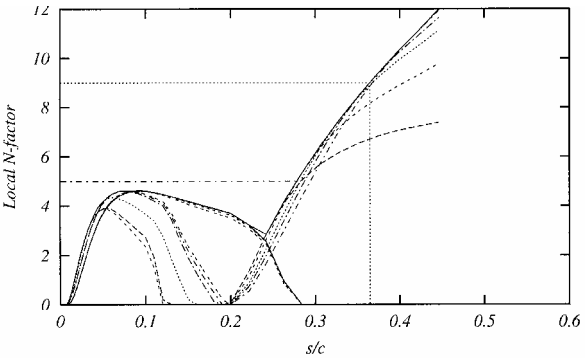


**Figure 4. N-factors corresponding to pressure distribution in Fig. 1 and suction shown in Fig. 3.**

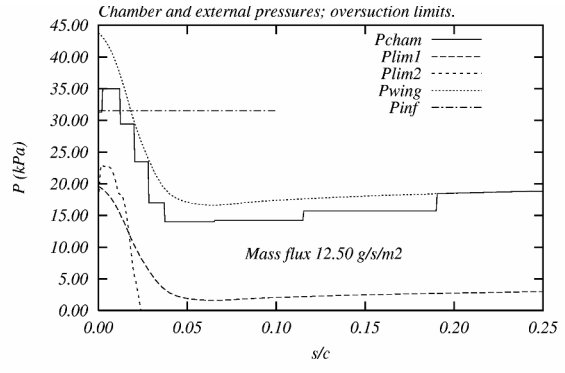


**Figure 5. External and plenum chamber pressures used to match suction distribution in Fig. 3.**

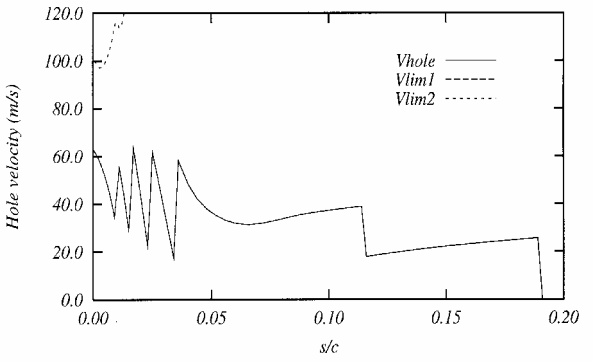


**Figure 6. Hole velocity distribution corresponding to Fig. 5.**

Porous surfaces cannot easily implement arbitrary distributions of transpiration velocity, so an attempt is made to match the trapezoidal transpiration velocity distribution with discrete but contiguous suction panels and plenum chambers. Figure 5 again shows the pressure variation over the upper surface of the wing, but in dimensional form and only over the suction region. Also on the figure is a set of eight discrete plenum pressure levels designed to effect the trapezoidal transpiration distribution shown in Figure 3; the actual resultant hole velocity distribution is shown in Figure 6. The distribution is very jagged near the leading edge because of the (necessarily) finite chamber lengths and the external pressure gradient. Although it is recognizably close to the distribution in Fig. 4, the aerodynamic constraints met by the analytical suction distribution are not reliably met by the chamber design. In this case the N-factors (not shown) exceed the suction-zone limit by about 20%. However the approach can always be improved in this respect by using a larger number of smaller chambers.

### B. Over-suction

Figures 5 and 6 also plot the chamber pressure over-suction limits *Plim1 & 2* and corresponding hole velocity limits *Vlim1 & 2* (i.e. limits beyond which transition would be accelerated by suction rather than delayed). The over-suction phenomenon is discussed more fully in Ref. 2: the first limit is a simple restriction on the Mach number of the flow through the suction holes; the second limit is more complex in form but is a measure of the disruptive effect of the hole suction on the local flowfield. The criteria used here were adapted from the results of two recent experimental investigations carried out by Reneaux & Blanchard[9] at ONERA and by Ellis & Poll[10] at Manchester University. Again, the over-suction phenomenon has been insufficiently researched at high Reynolds numbers and requires further attention.

### C. New approach

The approach described above has been used extensively and continues to be proposed for new designs. However, any kind of parametric study of Reynolds and Mach number variations, or changes to section and planform geometry, would require the chamber positions to be controlled; and this would effectively render the velocity-matching technique unworkable. For this reason, and in the light of the robustness of the aerodynamic methods involved, we decided to dispense with the analytical velocity distribution and manipulate the plenum pressures directly, measuring the response of the N-factor distribution to the plenum chamber pressures and adjusting the latter accordingly to satisfy the desired N-factor constraints. The process is described in some detail in Ref. 2 but a simplified flow chart is shown in Fig. 7.

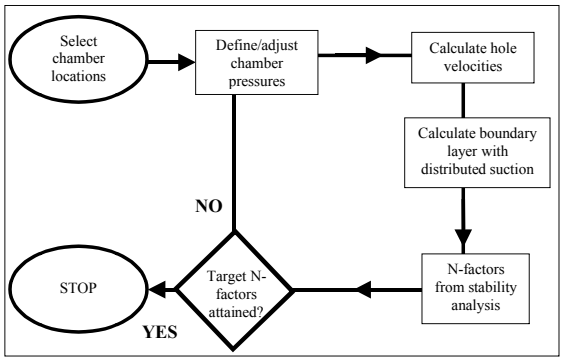


**Figure 7. Plenum pressure control process.**

An important part of this process is determining the relationship between the pressure drop across the porous skin and the resulting velocity through the holes (and thence the transpiration boundary condition for the laminar boundary layer calculation). The exact relationship used in this work was that derived by Preist and Paluch[12]. Over-suction constraints and additional requirements (such as attachment line stabilization) were also taken into account.

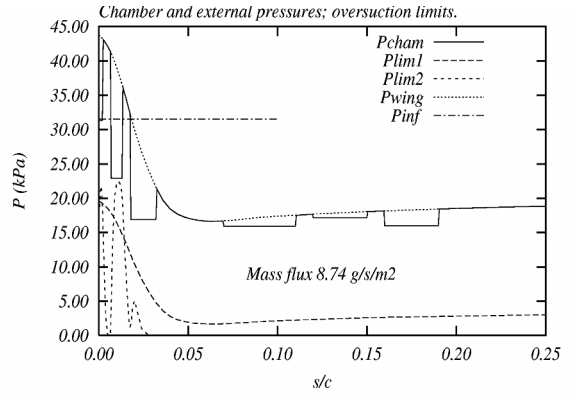


**Figure 8. Plenum pressure distribution obtained using the chamber design tool.**

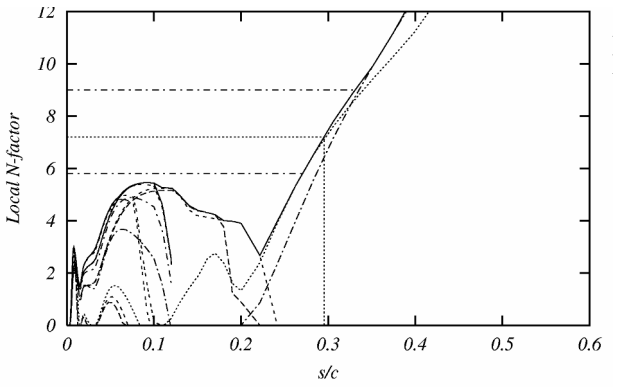


**Figure 9. N-factors corresponding to Fig. 8.**

The end result of the process is a chamber pressure specification which observes the N-factor constraints for each control region, as illustrated in Figures 8 and 9 (in this case for a six-chamber arrangement). This chamber layout was arrived at after only four or five design cycles. The first observation is that the tool has allowed the chamber positions to be optimized for efficiency quite rapidly, with the result that there is no chamber in the vicinity of the suction peak in the sectional pressure distribution. At this point in the flow the CF modes are stabilized by the changing external pressure gradient, while the TS modes are not yet unstable: suction is therefore least effective in this region. This may seem obvious with hindsight, but it became immediately apparent when examining the sensitivity of the N-factors to suction in this region. The second observation is that the suction rates in the leading edge region tend to be as large as permissible by the over-suction criteria, so that there is an implied benefit in gaining a better understanding the over-suction phenomenon. Thirdly, the overall velocity distribution is considerably different from the originally-proposed trapezium and includes gaps between the suction panels. Finally, savings are achieved of 20% in mass flow rate and 10% in plenum pressure difference (relative to free stream static pressure *Pinf*). These outputs can be used directly to determine savings in pump power, system weight and system cost.

The chamber design tool delivers just one of a number of possible solutions to the control problem (for a given chamber layout), but once an initial solution is obtained it is easy to adjust chamber pressures manually to investigate improved solutions. This usually involves increasing the suction levels at the upstream chambers, if possible. The process is also generally robust, thanks largely to the quality of the underlying analysis tools, although it would benefit enormously from the use of modern adjoint methods to calculate the required sensitivities. At the time the work was carried out the whole process would take between one and four hours on a Pentium 2, 350 MHz, processor depending on the number of chambers involved. A single control loop would involve the calculation of between 5000 and 30,000 eigenvalues. Clearly there would be enormous opportunities for the replacement of the full $e^N$ stability analysis with a robust, validated database-type method.

## III. Impact on predicted HLFC performance of aerodynamic assumptions and tools

The dependence of the suction system specification upon the 'control N-factor' constraint is as significant for the chamber-based design as it is for the trapezoidal transpiration distribution. Since this constraint mainly applies to CF instability modes, it might prove interesting to see how the use of a non-parallel stability method such as linear PSE[11] would impact upon the suction requirements: one of the main characteristics of linear PSE methods is the modelling of the stabilizing effect of convex surface curvature. The chamber design tool was therefore coupled to a PSE method written by Mughal at Imperial College[12] in place of the QinetiQ $e^N$ method 'CoDS'. The PSE N-factors were used to control the chamber pressures in the same way as before. Although at that time the N-factors from PSE analysis had not yet been rigorously calibrated against experimental data (at least in Europe), there was no evidence to suggest that transition N-factors would be markedly different. Applying the same N-factor constraint over the suction panels, however, did produce markedly different suction rates. The resulting chamber pressures shown in Fig. 10 are decidedly different from those shown in Fig. 8, yet the N-factor constraint is still satisfied, Fig. 11. The reason for this is that convex curvature in the region of the wing leading edge tends to stabilize CF modes appreciably. The question is which N-factor constraint is the more appropriate. If the PSE N-factors are used, the suction requirement in the leading edge region is significantly reduced, even necessitating a reduction in chamber

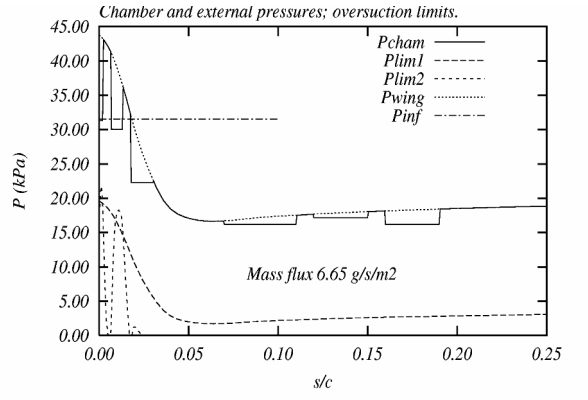


**Figure 10. Plenum pressures obtained using PSE stability analysis.**

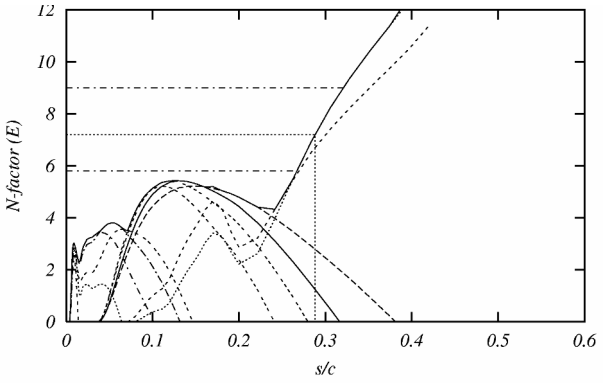


**Figure 11. PSE N-factors corresponding to the chamber layout shown in Fig. 10.**

sizes. The net effect is a 24% reduction in mass flow rate and, perhaps more significantly, the suction rates near the leading edge are now some way from the over-suction limit *Plim2* discussed earlier: this means a more conservative and less risky design.

## IV. Aerodynamic analysis of a complete wing with part-span HLFC

Having demonstrated the potential for significant (favourable) revisions to the transpiration requirements, the next objective was to apply the analysis to a three-dimensional wing and to assess the improvement in performance for the complete aircraft.

### A. Outline of the approach

Since the methods used for HLFC design are still very much restricted to quasi-two-dimensional flows (infinite-yawed or swept-tapered wings) the coupling of these methods with a fully three-dimensional CFD method was not considered. Instead, use was made of an existing QinetiQ tool[†] to construct a three-dimensional wing performance model from a set of swept-tapered boundary layer 'strips'.

Unlike the previous 2D studies, the effect of the pressure distribution and Reynolds number variation along the span must now be taken into account. The 2D-to-3D transformation code uses a simple outline of the wing and fuselage planform geometry to define the spanwise distribution of section lift coefficient $C_{L,sec}$ and Reynolds number for each of a series of wing-fuselage lift coefficients $C_{L,w+f}$. In principle (for the fully-turbulent case) Reynolds number dependence can be treated using simple power laws to scale the friction, form and wave drag. In this way the variation of the flowfield along the wing span can be obtained from a single lift-drag polar for the reference wing section. When there is a significant region of laminar flow the drag varies with Reynolds number in a non-trivial way. However the same 2D strip approach can be followed by calculating a series of polars for HLFC sections at different Reynolds numbers — Reynolds number sensitivity is then obtained from a database of results rather than from simple power laws.

Variation in overall aircraft lift coefficient can also be extracted from a single sectional polar. Because of the presence of the suction system, the influence of altitude is more complex than a simple Reynolds number effect, so the 2D-to-3D analysis has to be repeated for different cruise altitudes.

### B. Transformation to 3D

The first step of the transformation process was to analyze the baseline (turbulent) configuration at a given cruise altitude and Mach number. The representative wing section was transformed into an 'equivalent' two-dimensional aerofoil prior to calculating a 2D lift-drag polar. (The QinetiQ 2D viscous full potential code 'BVGK'[13] was used in the present work: BVGK not only calculates the 2D flowfield but also determines the lift, pitching moment and drag coefficients, the latter decomposed into friction, form and wave drag components.) At this stage, transition was set at 1% chord representing a standard 'turbulent wing' design and the 2D Reynolds number was set to a typical mid-span value.

[†] Developed by K. C. Hackett, QinetiQ Ltd.

At each spanwise station the 2D lift-drag polar was used to determine the local pitching moment and drag coefficients corresponding to the local 3D $C_{L,sec}$. The sectional pitching moment and drag distributions were then integrated over the span to give values for the wing-fuselage combination. These were then corrected empirically for additional factors, such as wing-off and interference drag, tail area and tail arm, to give overall coefficients for the trimmed aircraft. Repeated analyses at different values of $C_{L,w+f}$ yielded an overall lift-drag polar for the complete aircraft, $C_{D,a/c}$ versus $C_{L,a/c}$. Clearly there is a degree of empiricism built in to this approach, but the important point is that, by following the same procedure for the HLFC case, a sensible *comparison* can be made between the turbulent and HLFC aircraft.

For the HLFC cases the 2D-to-3D transformation procedure was modified by supplying additional 2D lift-drag polars for the HLFC wing sections. The application of the chamber design procedure to all the 2D HLFC cases was the expensive part of the analysis! Since each combination of chamber layout, $C_{L,sec}$, Reynolds number, Mach number and cruise altitude required a separate sectional HLFC analysis, a certain amount of scoping was done to establish the minimum number of combinations required for acceptable accuracy. The following constraints were applied in the present work, and seemed to limit the effort involved in the analysis without compromising either the accuracy or the significance of the results. First, a fixed chamber layout (i.e. chamber positions scaling with local chord) was imposed for a given configuration. Second, following a thorough investigation, it became clear that as few as three different values of section loading $C_{L,sec}$ would suffice to resolve adequately the 2D lift-drag behaviour at cruise (not counting the zero-lift case which would be common to both turbulent and HLFC polars): thus the pressure distribution shown in Fig. 1 was used along with two other cases developing 20% greater and less lift respectively. Third, spanwise variations in Reynolds number were treated by calculating polars at only two spanwise sections, the inboard and outboard extremes of the HLFC region, and using simple interpolation to obtain results for intermediate values. Fourth, a single cruise Mach number was chosen for the analysis, namely 0.8. Fifth, as with local Reynolds number variation, altitude effects were handled by analyzing each configuration at two extremes of altitude, typically 10,000 ft apart. This gave a total of four polars (two per cruise altitude), or twelve swept-tapered HLFC cases, for each configuration. The chamber design tool described above was used to determine chamber pressures, mass flow rates and an upper surface transition position for each of these twelve cases.

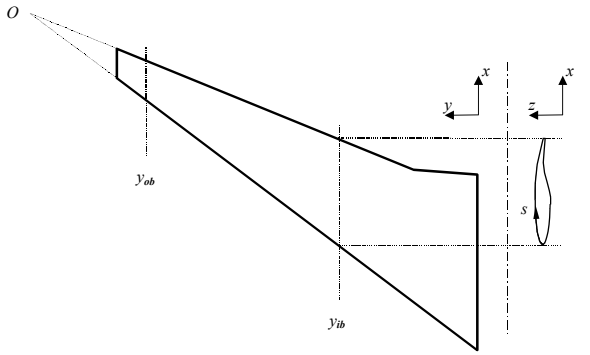


**Figure 12. Wing planform view illustrating the limits of HLFC application.**

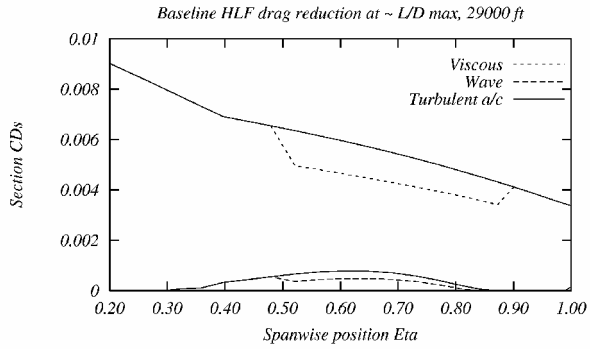


**Figure 13. Spanwise distribution of wing drag.**

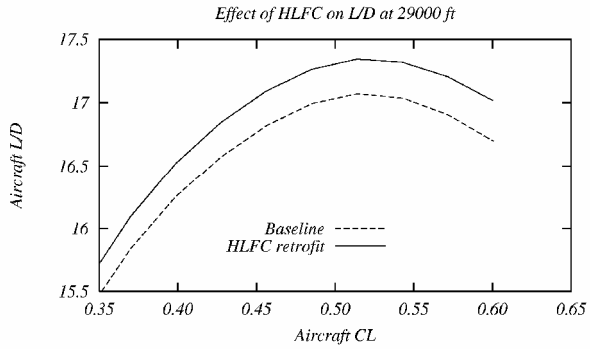


**Figure 14. Effect of HLFC retrofit on overall L/D.**

## C. Results

The following paragraphs present the results for the drag reduction for a medium-sized wide-body aircraft with a part-span HLFC retrofit (between 50% and 90% semi-span) on the wing *upper surface* only, as illustrated in Fig. 12. The spanwise distribution of drag reduction is shown in Fig. 13 at 29,000 ft and at the condition of maximum overall L/D: the observed reduction in viscous drag (about 20%) over the HLFC region is consistent with a rough estimate of 0.3 (delay in transition of 30% chord) × 0.67 (the proportion of viscous drag associated with the upper surface) ≈ 0.2.

Finally, the overall effect is summarized in Fig. 14 which focusses on the area around maximum L/D as predicted by the 3D performance estimation tool. The

difference between the baseline and HLFC retrofit aircraft represents an improvement in maximum L/D of 1.58% — this from laminarization of about 8½% of the wing upper surface. The results shown were obtained at 29,000 ft: the drag reduction at 39,000 ft is similar, but the overall aircraft drag coefficient is slightly greater, and the net benefit is only 1.46%.

## V. Performance penalties

### A. Pump drag analysis

The next task was to estimate the suction system power requirement and the effect on the overall aircraft performance, preferably in terms of an effective 'pump drag'. The analysis is described in detail in Ref. 3 and focusses on a control volume which encloses the pumped air from its initial state, in some notional streamtube ahead of the wing, to its final state as an exhaust jet, Fig. 15.

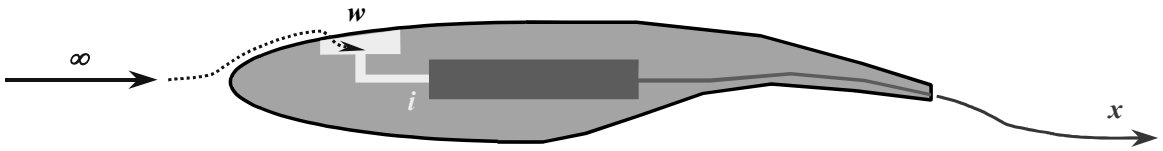


**Figure 15. Schematic of pumped air flow process (see Nomenclature for definition of states ∞, *w*, *i* and *x*).**

Taking into account the finite efficiency of the various thermodynamic processes involved in pumping the air, and allowing for the net thrust developed as the sucked air is expelled, the overall 'pump drag' penalty can be expressed as:

$$D_{pump} = \frac{\left[\eta_{a/c} \big/ \eta_{off}\right]}{\eta_{motor}\eta_{pump}} \frac{\dot{m} c_p T_{0i}}{u_\infty} \left[ \left( \frac{p_\infty}{p_{0i}} \right)^{\frac{\gamma-1}{\gamma}} \left( 1 + \frac{\gamma-1}{2} M_x^2 \right) - 1 \right] - \dot{m}\left(u_x - u_\infty\right) \tag{1}$$

Values for pump and motor efficiencies were suggested by one of the HYLTEC project partners the with systems expertise[‡]. More difficulty was encountered in finding a figure for the relative power off-take efficiency ratio, $[\eta_{a/c}/\eta_{off}]$, and a value of 0.8 was assumed for the present study (i.e. power off-take was assumed to be more efficient than the propulsive process).

The principal variables in the present problem were the total mass flow rate and the increase in total pressure required from pump inlet to pump exhaust. Conveniently, these are the quantities yielded by the 2D section design tool described earlier. Although the resulting suction chamber plenum pressures were by no means uniform, the present analysis was simplified by assuming that the streams from all chambers would be throttled down to the lowest common pressure. The problem of $C_{L,sec}$ variation across the span was mitigated by the fact that, at the lower value of lift coefficient, both chamber pressures *and* mass flow rates were lower — the converse being true at the higher value of $C_{L,sec}$. The resulting variation in pump drag was less than 4%. Finally, Reynolds number variation across the span was treated by *averaging* the local values of mass flow rate at mid-span and tip, while taking the *minimum* of the chamber plenum pressures. In all cases the effects of these simplifications were small and would not influence the overall conclusions.

Using equation (1) above the pump drag penalty for the six-chamber layout shown in Fig.8, derived using a classical $e^N$ approach, would be about 0.24% of total drag for the specimen aircraft operating at maximum *L/D,* Mach 0.8 and 29,000 ft (the figure is almost identical for 39,000 ft). This compares with the previously quoted aerodynamic drag reduction of 1.58% — so that the pump drag penalty amounts to about *one sixth* of the drag reduction. The pump drag penalty for the suction system designed on the basis of PSE N-factors diminishes to only 0.18% of total drag. Both results compare very favourably with the simple trapezium-shaped suction distribution of

[‡] H. Sturm, AoA Gauting, Germany.

Figures 5 and 6, which requires nearly 50% more mass flow and a greater pump pressure rise: the calculated pump drag then becomes 0.40% of total aircraft drag at maximum *L/D*, over one quarter of the HLFC benefit.

A popular issue among the HLFC research community is the optimization of exhaust Mach number to reduce the overall pump drag. In the case of unit efficiencies, the classical optimum condition in which the exhaust velocity is equal to the free stream velocity can be derived easily from equation (1). However the effect of losses in the system is to flatten considerably the minimum in the pump-drag-versus-exhaust-Mach-number relationship. Thus, for example, the pump drag penalty for the mass flow rates discussed above is 0.24% at an exhaust Mach number of 0.2, but this only drops to a minimum of 0.22% when the exhaust Mach number is increased to 0.63. Since the overall impact of pump drag is rather small — *for a well-designed system* — optimizing exhaust velocity from a perspective of *drag* alone may be misleading since the exhaust velocity requirement also determines the size and *weight* of the required pump. These factors would impact significantly upon the ease of installation as well as the overall aircraft aerodynamics.

### B. System weight considerations

One remaining factor to be considered is the weight penalty associated with the ducting, pump and control equipment required for the suction system. Since the present work is concerned with changes in drag, it was thought useful to express the suction system weight estimates obtained during the HYLTEC project as additional drag penalties. This was done by considering the lift-drag trade-off at maximum *L/D*:

$$\Delta C_{D,cruise} \approx \frac{\Delta m}{m_{cruise}} \frac{C_{L,cruise}}{[L/D]_{cruise}} \tag{2}$$

On this basis an additional ‘weight penalty’ of 0.20% total aircraft drag should be added to the pump drag to obtain the overall performance penalty associated with the HLFC system. For the specimen aircraft, the *aerodynamic* drag reduction of 1.58% is then reduced to 1.14% overall. If the PSE N-factors are used for design this figure rises to 1.25%. For the case of the trapezium suction distribution the net benefit is only 0.89%. Here the system weight is assumed to scale more or less with suction mass flow rate.

## VI. Effect of constrained design modifications on HLFC performance.

Having developed the analysis of the preceding sections, the tools were then available to conduct a parametric study on wing geometry. Three incremental modifications to the wing section were investigated for their effect on the performance of both the turbulent and HLFC wing:

- a reduction of 2° in leading edge sweep;
- a reduction in section thickness over the first 20% of chord; and
- a positive 'flap' deflection (last 20% chord) of 2°.

The sweep reduction was expected to reduce the control requirements for crossflow instability. Both section geometry modifications shifted the sectional loading further aft, reducing the amplification of Tollmien-Schlichting waves downstream of the suction control region, but increasing the wave drag significantly compared to the HLFC benefit.

The results of these changes are summarized in Table 1 below. The sweep reduction did indeed reduce the amount of suction power required (and therefore pump drag) by about one tenth, without much impact on the extent of laminar flow. Since the pump drag penalty amounts to only one sixth of the overall HLFC benefit, this further improvement is perhaps insufficient to justify the effort of changing the wing geometry. The nose geometry modification did have a significant impact upon viscous drag saving since transition was delayed much further, to 38% chord or beyond. This was due to a more favourable pressure distribution which, unfortunately, was also the origin of the wave drag increase. The trailing edge deflection yielded very little benefit, except to make transition more responsive to additional suction by moving the shock further aft. In general, although there was some increase in laminar extent, most of these modifications resulted in significant wave drag penalties while making little impact upon the overall drag balance — certainly not enough to consider the cost of implementing such a geometry modification.

This was an interesting finding, and may prove to be a general rule with today's advanced wing section designs which are highly-optimized from the point of view of wave drag. Admittedly, the balance might change if a greater span of the wing were laminarized, but it appears from these studies that far more benefit is likely to come from extending the suction control region further downstream than by trying to pursue a 'laminar flow section' design philosophy for future HLFC applications.

**Table 1: summary of HLFC benefit, pump drag penalty and net benefit for baseline wing geometry and various modifications.**

| Case no. | Details of any geometry modification | HLF analysis details | -ΔCD (Aero) %total | ΔCD (Pump) %total | ΔCD (Weight) %total | -ΔCD (net) %total |
|---|---|---|---|---|---|---|
| 1T | Baseline | Turbulent baseline investigated at 29,000 ft, Mach 0.8, using a 2D->3D analysis at maximum L/D. | **0.00%** | | | |
| 1L | Baseline | HLFC on upper surface between 50% and 90% semi-span. Transition between 29% - 34% chord. | **1.58%** | **0.24%** | **0.20%** | **1.14%** |
| 2T | Reduced sweep | As for case 1T. | **-0.68%** | | | |
| 2L | Reduced sweep | As for case 1L. Transition between 31% - 42% chord. | **1.12%** | **0.21%** | **0.20%** | **0.71%** |
| 3T | Reduced nose thickness | As for case 1T. | **-0.42%** | | | |
| 3L | Reduced nose thickness | As for case 1L. Transition between 29% - 46% chord. | **1.67%** | **0.17%** | **0.20%** | **1.30%** |
| 4T | Negative flap | As for case 1T. | **-0.59%** | | | |
| 4L | Negative flap | As for case 1L. Transition between 22% - 32% chord. | **1.09%** | **0.24%** | **0.20%** | **0.65%** |

## VII. Conclusions

An automatic tool has been developed to facilitate HLFC design by satisfying N-factor constraints through iterative adjustment of plenum chamber pressures. The method relies on the existence of a robust, 'black-box' boundary layer and stability analysis methods. The new approach has highlighted some of the deficiencies of the fixed-velocity-distribution approach. The importance of modelling the actual control technique (e.g. transpiration through a porous wing skin) is perhaps a useful message to those who are developing analytical suction optimization tools for HLFC design.

An N-factor control philosophy has been proposed which attempts to balance the technical risk of an HLFC system against system power and weight penalties. The philosophy is limited by the onset of non-linear behaviour, and the consequent failure of the $e^N$ model. The philosophy must be properly validated and/or modified with further research, particularly in the area of non-local and non-linear analysis of crossflow instability, since it dictates about 50% of the mass flow requirements — at least for the test case presented here. Further research is required on the over-suction phenomenon, particularly in the highly swept flow close to an attachment line where the over-suction problem appears to have the greatest impact on high-Reynolds-number HLFC design.

The HLFC wing section designs of previous studies have been successfully combined, using a 2D-to-3D transformation tool, to allow the performance of a complete wing with part-span HLFC retrofit to be assessed. For a laminarized area equal to 8½% of the wing upper surface, an aerodynamic drag benefit of 1.6% total aircraft drag is predicted at maximum *L/D*. System weight and power requirements suggest that the net benefit would be reduced to 1.1% total aircraft drag. PSE methods would appear to predict more modest suction requirements for stabilization of crossflow modes, increasing the net benefit to 1.3% of total aircraft drag. Simple trapezoidal velocity distributions applied without reference to local N-factor sensitivities would reduce the benefit to 0.9% of total drag.

Modifications to the wing geometry indicate that changes favourable to laminar flow nevertheless introduce unacceptably large wave drag penalties. The most promising direction for future design research appears to be extending the extent of the suction control system in both spanwise and chordwise directions, and to other parts of the airframe: the surface area subjected to HLFC retrofit in the present study amounts to only 18% of the combined area of wing upper surface, tailplane and fin. A similar HLFC performance in all these areas would suggest a potential 6½ - 7% reduction of total aircraft drag for the specimen aircraft at cruise.

## Acknowledgments

The author would like to thank the UK Department of Trade and Industry and the European Commission for their financial support, and the other HYLTEC project partners for their co-operation and valuable contribution to this study.

## References

[1]Bieler, H., "HYLTEC Hybrid Laminar Flow Technology. Annex 1: Project Programme", Technical Annex to European Commission contract no. BRPR-CT97-0606, November 1997.

[2]Atkin, C. J., "New Aerodynamic Approach to Suction System Design", *Aerodynamic Drag Reduction Technologies*, Notes on Numerical Fluid Mechanics, Vol. 76, edited by P. Thiede, Springer, Berlin, 2001, pp. 55-63.

[3]Atkin, C. J., and Courtenay W. J. A., "Predicting the cruise performance of a retrofit Hybrid Laminar Flow Control system", *CEAS Aerodynamics Conference*, Cambridge, United Kingdom, June 2002.

[4]Atkin, C. J., "Calculation of laminar boundary layers on swept-tapered wings", QinetiQ Ltd. Report FST/TR025107, February 2004.

[5]Horton, H. P., and Stock, H. W. "Computation of compressible, laminar boundary layers on swept, tapered wings", *J Aircraft*, Vol. 32, No. 6, 1995, pp. 1402,1405.

[6]Atkin, C. J., and Poll, D. I. A., "Correlation between linear stability analysis and crossflow transition near an attachment line", *Transitional Boundary Layers in Aeronautics*, edited by R.A.W.M. Henkes and J.L. van Ingen, North-Holland, Amsterdam, 1996, pp. 155-164.

[7]Mack, L. M., "Boundary layer stability theory", AGARD Report 709, Chapter 3, 1984.

[8]Schrauf, G., Perraud, J., Lam, F., Stock, H. W., Vitiello, D., and Abbas, A., "Transition prediction with linear stability theory – lessons learned from the ELFIN F100 flight demonstrator", *2nd European Forum on Laminar Flow Technology*, Bordeaux, June 1996.

[9]Reneaux, J., and Blanchard, A., "The design and testing of an airfoil with hybrid laminar flow control", *1st European Forum on Laminar Flow Technology*, Hamburg, March 1992.

[10]Ellis, J. E., and Poll, D. I. A., "Laminar and laminarizing boundary layers by suction through perforated plates", *2nd European Forum on Laminar Flow Technology*, Bordeaux, June 1996.

[11]Herbert, T., "Parabolised stability equations", AGARD Report 793, Chapter 4, 1994.

[12]Mughal, M. S., and Hall, P., "Parabolized stability equations and transition prediction for compressible swept-wing flows", Imperial College Report, November 1996.

[13]Ashill, P. R., Wood, R. F., and Weeks, D. J., "An improved, semi-inverse method of the viscous Garabedian and Korn method (VGK)", RAE TR 87002, 1987.

[14]Preist, J., and Paluch, B., "Design specification and inspection of perforated panels for HLFC suction systems", *2nd European Forum on Laminar Flow Technology*, Bordeaux, June 1996.